(26) Schaefer, J. *Macromolecules* **1973**, *6*, 882.
(27) Valeur, B.; Monnerie, L. *J. Polym. Sci., Polym. Phys. Ed.* **1976**, *14*, 11.
(28) Morgan, R. J.; Nielsen, L. E.; Buchdahl, R. *J. Appl. Phys.* **1971**, *42*, 4653.
(29) Weber, G.; Tormala, P. *Colloid Polym. Sci.* **1978**, 256, 638.
(30) Ueno, H.; Otsuka, S.; Kushimoto, A. *Kobunshi Ronbunshu* **1978**, *35*, 339.
(31) Smith, P. M.; Boyer, R. F.; Kumler, P. L. *Macromolecules* **1979**, *12*, 61.

# Polymeric Materials from the Gel State. The Development of Fringed Micelle Structure in a Glass

**Steve Wellinghoff,* Julie Shaw, and Eric Baer**

*Department of Macromolecular Science, Case Western Reserve University, Cleveland, Ohio 44106.* *Received December 26, 1979*

ABSTRACT: Rapid cooling of concentrated solutions of atactic (APS) and isotactic (IPS) polystyrene and poly(2,6-dimethylphenylene oxide) in low molecular weight solvents yields gels which are cross-linked by small 20–100 Å fringed micelle crystallites and/or glassy microdomains. The crystal size and perfection and microphase separation in glasses of PS, PPO, and their blends cast from gel solution are affected by the gelation solvent and annealing treatement. The IPS gel crystals consist of a high-energy conformational variant of the usual isotactic configuration, while the normal $4_1$ helical tetragonal form of PPO was found for its gel crystals. These gel glasses are useful for exploring, in a controlled way, the effect of microheterogeneity on localized plastic deformation.

The region below the binodal in the phase diagram of a two-phase system exhibiting an upper critical solution temperature (UCST) can be divided into two parts, namely, a metastable region between the binodal and the spinodal and an unstable region below the spinodal.[1] In the metastable region, minimization of the free energy of the system requires that large excursions in concentrations about the average occur in neighboring regions. The large composition difference that exists across the phase interface is responsible for a relatively large surface free energy. Thus, in this region, phase separation is reminiscent of crystal nucleation and growth, and isolated particles will nucleate and continue to grow at the same internal composition until they are large enough to scatter light. Typically, polymer solutions will exhibit this type of behavior near the Θ temperature.

If the mobility of the system is sufficiently low and if the solution is quenched rapidly to a temperature below the spinodal line, nucleation and growth can be avoided, and the solution can phase separate by a spinodal mechanism. Since within this region the curvature of the free energy of the system with respect to composition is negative, even infinitesimal concentration fluctuations will continue to grow. Provided that the volume fraction of the minor component is high enough, the microphase morphology will consist of two continuous interconnected phases separated by a characteristic distance. In the initial stages of microphase separation, the same characteristic interphase distance will be maintained as the two phases diverge in composition with increasing time. If one of the phases is a polymer-rich phase, the morphology will be frozen in as soon as the polymer concentration increases enough to cause the $T_g$ of this phase to be below the temperature of phase separation. Macroscopically, this system will exhibit rubbery, gelatinous characteristics as a consequence of the low mobility within the interconnected polymer-rich phase.

Concentrated (>5–10%) solutions of APS in decalin will phase separate into opaque gels at ca. 10 °C;[2] turbid, freely-flowing solutions develop at lower concentrations. The polystyrene self-associations that promulgate phase separation do not appear suddenly at the CST. Shear flow experiments can detect these associations at temperatures as high as 40 °C in decalin solutions which are quite clear.[3]

If the polymer is crystallizable, the concentration gradients that occur in the neighborhood of the CST will often be sufficient to induce polymer crystallization. In the case of spinodal phase separation, the crystallites that form in the polymer-rich phase can immobolize polymer chains in the network and stabilize the phase separation at a domain size below that required for the scattering of visible light. For example, isotactic PS (IPS)–decalin solutions form clear gels at <15 °C,[4] quite close to the UCST of 10 °C. Cross-links composed of 100-Å fringed micelle crystals were found to be responsible for the rubbery behavior of the solution. Paul[5] has summarized many other polymer–solvent systems that undergo the phenomenon of thermally reversible gelation. The observed decrease in melting point of the gel as the difference between the Hildebrand solubility parameters of the polymer and solvent decreased led him to suggest that gelation might be predicted by a thermodynamic theory of phase separation provided that surface energy contributions arising from the very small sizes of the phase were taken into account.

We were interested in these gel systems because they provided a route for making glassy polymer films containing well-defined crystalline heterogeneities of ca. 100 Å in size. These would be formed in a spinodally-phase-separating system of constant interphase distance. Heterogeneities of this dimension are thought to have a profound influence on the development of localized plastic deformation.[6] In addition, this glass morphology clearly avoids the complicated structure-property correlations that would attend a spherulitic structure and minimizes the uncertainty in heterogeneity that would otherwise exist in a completely amorphous glass. This paper concentrates on the preparation and structural characterization of polystyrene (PS), poly(2,6-dimethylphenylene oxide) (PPO), and PS–PPO glasses cast from gelled solutions. A subsequent report will discuss the plastic deformation behavior of these materials and its relationship to the heterogeneities introduced into the glass.

## Experimental Section

Additive-free PPO ($M_v \simeq 25\,000$; General Electric Co.), narrow-fraction, atactic polystyrenes (APS's) ($M_n$ = 4000, 37 000,

0024-9297/79/2212-0932$01.00/0 

200000, 670000, 2000000; $M_w/M_n \simeq 1.05$; Pressure Chemical Co.), and isotactic polystyrene (IPS) ($M_w \simeq 670000$) were used for this study. The IPS was purified by methyl ethyl ketone extraction and was shown by $C^{13}$ NMR to be greater than 98% isotactic. All of the solvents used were at least of AR grade and were dried over phosphorus pentoxide.

Gels were produced by dissolving the polymer into the chosen solvent and cooling the solution down to the gelation temperature for a time sufficient to yield a rubbery solution. Glassy films were produced by first evaporating the solvent under vacuum and then removing the residual solvent by extracting it with a low-boiling exchange solvent such as acetone, isopentane, or hexane. The microstructure of these materials was characterized by FTIR (Digilab), calorimetric (Perkin-Elmer DSC II), and X-ray (GE diffractometer, Statton flat plate camera) measurements.

Gel melting points were determined visually by gelling the solutions in test tubes which had been tilted, increasing the temperature, and observing when the gel in upright test tubes would begin to flow under its own weight forming a level meniscus.

The percentage of polymer contained in the crystalline form in a gel glass film of a known thickness was calculated by using the FTIR capability to digitally subtract a standard, completely-amorphous polymer of a known film thickness until a completely crystalline spectrum had been isolated. Of course, knowledge of percent crystallinity allowed calculation of absolute heats of melting for the same film.

## Results and Discussion

**A. Phase Separation and Gelation. 1. Atactic Polystyrene Solutions.** Study of the gelation phenomenon in the absence of crystallization required the use of APS fractions. The large refractive index difference between APS and $CS_2$ made this polymer solvent system ideal for visual observation of phase separation. Θ temperatures were observed for 0.3% volume fractions of mol wt 37000, 200000, 670000 in $CS_2$ between −108 and −94 °C, while a precipitate formed in the mol wt 2000000 polymer between −94 and −78 °C. A clear gel was formed in 1.0% mol wt 2000000 and 670000 APS solutions upon cooling to the same temperature (−94 °C). Both the gel formation temperature and gel melting temperature increased with increasing polymer volume fraction. For example, although a 16% solution of mol wt 37000 APS would gel at −35 °C, a 10% solution would not gel until −78 °C; the visual melting point decreased from −20 to −40 °C in the same order (Figure 1A). Molecular weight also had a strong effect upon the gel melting point in that $T_m$ increased from −25 to +5 °C as the molecular weight increased from 4000 to 670000 (Figure 1B).

Crystallization was definitely not the cause of gelation in the APS–$CS_2$ system since high-sensitivity DSC measurements on these solutions revealed neither endothermic nor exothermic peaks. Additionally, the IR spectra of APS–$CS_2$ solutions showed no significant changes upon cooling to −78 °C.[12,13] The lack of any detectable difference in the FTIR spectra of APS glasses cast at −78 and 25 °C also supported the contention that crystallization was not the source of gelation.

The remaining possibility of course is that quenching the solution into the unstable region yielded a fine dispersion of polymer-rich regions whose $T_g$ was sufficiently low to pin different polymer chain ends in the same glassy particle. The small size of these domains (<1000 Å as indicated by the gel clarity) and the rapidity of their formation (<1 min) suggest that they develop by the spinodal mechanism.

The critical point (maximum) in the binodal of a polymer solvent system usually appears around 5–15% polymer volume fraction.[8] Since the shape of the composition vs. gel-melting curve in Figure 1A obviously does not comply, the melting of the gel must be a consequence

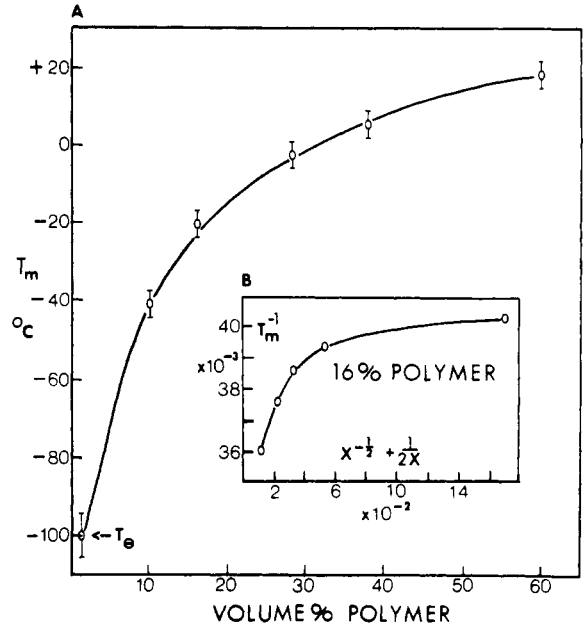


**Figure 1.** (A) Gel to mobile transition temperature, $T_m$, as a function of volume fraction of a mol wt 37000 APS in $CS_2$. (B) $T_m^{-1}$ vs. $X^{-1/2} + (1/2X)$ of a 0.16 volume fraction of various narrow fraction molecular weight APS's in $CS_2$ (X ≡ degree of polymerization).

of factors other than crossing of a coexistence line. The most likely explanation is that when the gel is heated, the $T_g$ of the phase-separated glassy domains is surpassed, freeing the polymer chains that were originally cross-linked by these structures. This hypothesis is also supported by Figure 1B, which shows that $T_m$ is not a linear function of Flory's molecular weight parameter ($X^{-1/2} + (1/2X)$; $X$ ≡ degree of polymerization); of course, linearity would identify $T_m$ with the binodal. At higher temperatures, only a few domains containing the highest polymer volume fractions, and consequently having the highest $T_g$, would remain glassy. However, there are evidently a sufficient number of these to maintain a three-dimensional network for the longer molecules. Unfortunately, the location of the actual binodal cannot be determined except to say that the curve in Figure 1A represents the minimum possible binodal temperature at each composition.

Solutions of 16% volume fraction of mol wt 37000, 200000, 670000 APS in aniline formed solid clear gels at −35 °C; the mol wt 200000 PS gel melted at −25 °C. Benzaldehyde solutions of the same molecular weights also formed clear solutions which would not flow under their own weight at −78 °C. However, these solutions just became more plastic as temperature was increased and no distinct melting point was detected. Decalin solutions of APS fractions of the same concentration phase separated yielding the opaque brittle precipitate characteristic of a nucleation and growth mechanism.[2]

**2. Isotactic Polystyrene Solutions.** Table I shows that clear rubbery gels can be formed from 10% solutions of IPS in seven solvents; a number of these gels, especially those formed from 1-chlorododecane and 1-chlorodecane solutions, became opaque upon standing above 25 °C. Diethyl oxalate solutions yielded an opaque gel as soon as the temperature was lowered to 100 °C. The very high melting point (190 °C) of the diethyl oxalate gel relative to the melting point of the clear gels formed at lower temperatures suggested that a more stable crystal structure was responsible for both the opacity and the high melting point. In fact, the gel melting point of 1-chlorododecane gels increased from 88 to 180 °C upon the development

Table I
Correlation of IPS Gel Crystallization with Phase Separation[a]

| solvent | $\delta_T$ | $\delta_D$ | $\delta_P$ | $(Q = 0)$ $V_1A_{12}$ | $(Q = 0.92)$ $V_1A_{12}$ | $T_\theta$, °C | $T_{GEL}^{IPS}$, °C | | $T_M^{IPS}$, °C |
|---|---|---|---|---|---|---|---|---|---|
| (1) diethyl oxalate | 8.6 | | | | | +37[b]; +24[c] | (100) | VC | (190) |
| (2) 1-chlorodecane | 8.2 | 8.1 | 1.5 | 437 | 437 | +43; +29 | +25 | C | +88 |
| (3) decalin | 8.8 | 8.8 | 0 | 240 | 240 | +15; +6 | +12 | C | +63 |
| (4) 1-chlorodecane | 8.3 | 8.2 | 1.5 | 325 | 325 | +20; +13 | +13 | C | +85 |
| (5) nitrobenzene | 10.6 | 9.2 | 6.5 | 2987 | 240 | | −2 | C | +52 |
| (6) aniline | 11.0 | 9.5 | 5.6 | 1845 | 149 | −30[d] | −20 | C | +5 |
| (7) benzaldehyde | 10.4 | 8.9 | 5.0 | 1575 | 176 | −40[d] | −35 | C | +20 |
| (8) acetophenone | 9.7 | 8.6 | 4.6 | 1507 | 188 | +21[fr] | sol to fr | | +25 (SW) |
| (9) benzonitrile | 10.8 | 9.7 | 4.8 | 1413 | 133 | −14[fr] | sol to fr | | +25 (SW) |
| (10) *o*-dichlorobenzene | 10.0 | 9.4 | 3.0 | 406 | 33 | −17[fr] | sol to fr | | +25 (D) |
| (11) 1-bromonaphthalene | 10.6 | 9.9 | 2.5 | 309 | 53 | −6[fr] | sol to fr | | +25 (D) |
| (12) 1-chloronaphthalene | 10.4 | | | | | −2[fr] | sol to fr | | +25 (D) |
| (13) *m*-dibromobenzene | 11.1 | | | | | −7[fr] | sol to fr | | +25 (D) |
| (14) 1-methylnaphthalene | 9.8 | | | | | −31[fr] | sol to fr | | +25 (D) |
| (15) toluene | 8.9 | 8.8 | 1.3 | 38 | 38 | −95[fr] | sol to fr | | +25 (D) |
| (16) carbon disulfide | 10.0 | 10.0 | 0 | 94 | 28 | −22[d] | −38 −63 | C | −21 |
| polystyrene | 9.5 | 9.4 | 1.1 | | | | | | |
| poly(phenylene oxide) | 9.8 | 9.4 | 2.7 | | | | | | |

[a] $V_1$ = molar volume (cm³/mol). $A_{12} = (\delta_{DS} - \delta_{DP})^2 + (1 - Q)(\delta_{AS} - \delta_{AP})^2$, S = solvent, P = IPS, PPO polymer. $\delta_T$ = total solubility parameter [(cal/cm³)$^{1/2}$]; $\delta_D$ = dispersive part; $\delta_P$ = polar part. Sol to fr means the solution that remained mobile and clear until the freezing point; SW means swelled gel glass prepared for decalin solution; D indicates dissolved glass prepared for decalin solution; C indicates a clear gel; SCL indicates a slightly cloudy gel; and VCL indicates a very cloudy gel. $T_{GEL}$ is the temperature at which gelation is instantaneous. $T_M$ is the gel melting point. fr is the freezing temperature. [b] Cloud point of narrow fraction mol wt 2 000 000 APS (0.3% concn). [c] Cloud point of narrow fraction mol wt 200 000 APS (0.3% concn). [d] Clear gel point of narrow fraction mol wt 2 000 000 APS (10% concn).

of opacity. The close proximity of the IPS gelation temperature to both the Θ temperature and the APS gelation temperature suggests that imminent microphase separation is a necessary condition for gel crystallization.

As the temperature is increased above the UCST, the formation of an IPS gel requires an increasingly longer time.[4] For example, although gelation occurs almost instantly in nitrobenzene solutions at −2 °C, it required 3 days at −5 °C when the UCST was lowered by the addition of 50% *m*-dibromobenzene. This behavior is characteristic of nucleation-controlled crystallization kinetics. Although significant microphase separation would not be expected at temperatures above the UCST, the transient intermolecular associations that still exist in noncrystallizable polymers at temperatures 20 °C above the UCST[3] might have a significant effect upon the crystallization process.

Upon studying the solution behavior of IPS in numerous solvents (Table I) of differing solubility parameter, we found that gel formation and melting temperatures could be correlated with the polymer–solvent endothermic interaction energy.[8,9] The larger the value of $A_{12}$, the more unfavorable the polymer solvent interaction and, consequently, the higher the UCST and the gel formation and melting temperature. Although no gelation was observed for solvents 8–15 because the solvent crystallized at temperatures higher than the gel-formation temperature, solvents 8 and 9 swelled an initially dry gel glass at 25 °C while solvents with lower $V_1A_{12}$ completely dissolved the gel glass, a result in line with the proposed correlation. Carbon disulfide solutions which had the smallest interaction energy did not gel until −38 to −63 °C. However, this correlation breaks down when the relatively nonpolar solvents, decalin, 1-chlorodecane, and 1-chlorododecane, are considered. For example, although nitrobenzene and decalin solutions gel at similar temperatures, their calculated interaction energy differs by a factor of 10. Since at the Θ temperature[8]

$$\chi = \chi_s + \frac{V_1A_{12}}{RT_\Theta} \qquad (1)$$

$$\chi_s \simeq 0.3\text{–}0.4; \quad \chi = 0.5$$

$V_1A_{12}$ values $>10^3$ cal are not realistic. Evidently, in the IPS gel system the polar contribution to the interaction energy is not as large as that envisioned in Hansen's[10] solubility parameter approach.

The same type of behavior is found for the nitrobenzene–toluene system. Heat of mixing data for the binary mixture obeys the relation[23]

$$\Delta H_m = A_{12}v_1v_2 \qquad (2)$$

where $A_{12} = (\delta^1 - \delta^2)^2 = [(\delta_d^1 - \delta_d^2)^2 + (\delta_p^1 - \delta_p^2)^2]$ and $v_1$ and $v_2$ are volume fractions of the two components. The value of $A_{12}$ which is found (+0.76 cal/cm³) is considerably less than would be calculated from the total solubility parameters ($A_{12}$ = 2.89 cal/cm³) or from Hansen's solubility parameter equation ($A_{12}$ = 27.02 cal/cm³). Exothermic heats of mixing have been found for binary mixtures of nitrobenzene with aniline, *m*-cresol, and *m*-xylene.[23] Clearly, some specific, favorable interaction between unlike molecules, possibly charge transfer,[24] is overcoming the positive energy contribution generated by the differences in cohesive energy density.

Since nitrobenzene–PS and decalin–PS solutions behave similarly, we assume that the polymer–solvent interaction energies for both systems are equal.

$$V_{decalin}[(\delta_d^{PS} - \delta_d^{DEC})^2 + (\delta_p^{PS} - \delta_p^{DEC})^2] = V_{PhNO_2}[(\delta_d^{PS} - \delta_d^{PhNO_2})^2 + (\delta_p^{PS} - \delta_p^{PhNO_2})^2 - Q(\delta_p^{PS} - \delta_p^{PhNO_2})^2] \qquad (3)$$

In order to take into account any favorable charge-transfer interaction between nitrobenzene and PS, we multiply the polar part of the interaction energy by a constant $Q$. Thus the charge-transfer interaction is assumed to be roughly proportional to the polar contribution to the energy and acts in opposition to the dipole–dipole interactions. Obviously, no charge transfer can occur between decalin and polystyrene and $Q$ = 0. As a further approximation, the $Q$ calculated from eq 3 is used to calculate a corrected $V_1A_{12}$ for the other solvent systems, with the exception of the chlorinated paraffins which probably have little or no

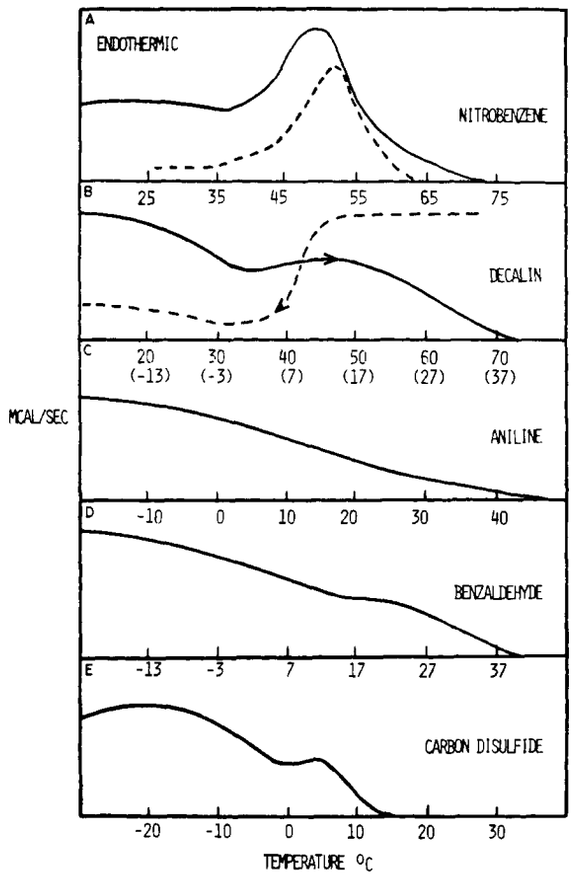


**Figure 2.** DSC scan at 20 °C/min of a 0.16 volume fraction IPS in various solvents (endothermic above abscissa): (a) gelled at −5 °C for 0.5 h and heated to 95 °C (solid line); after the gel was cooled again to −5 °C, it was heated to 37 °C, cooled at 180 °C/min to −5 °C, and immediately reheated (dotted line); (b) gelled at −10 °C for 5 min and heated to 100 °C (solid line); exothermic crystallization resulting from cooling at 10 °C/min from 130 °C (dotted line) (temperature of cooling run in parentheses); (c) gelled at −40 °C for 5 min and heated (solvent does not freeze at this polymer concentration); (d) gelled at −43 °C for 5 min and heated; (e) gelled at −50 °C for 5 min and heated.

charge-transfer interaction with an aromatic nucleus. Even this approximate treatment would break down if a strong acceptor (nitrobenzene) was being mixed with a strong donor (aniline).

In any case, the $V_1A_{12}$ values calculated using $Q = 0.92$ appear to more successfully predict the gelation behavior of IPS. The more successful correlation is obtained with the gel melting temperature. There are exceptions however, notably, the toluene–PS solution which is known to have a negative heat of mixing.[11]

**3. PPO Solutions.** The gelation behavior of PPO was also studied in the same series of solvents. High values of the interaction energy, $V_1A_{12}$, led to phase separation into an opaque gel at high temperatures (25–70 °C). Slightly cloudy or clear gels were found only in the case of the $\alpha$-substituted naphthalenes, a 50/50 mixture of *m*-dibromobenzene and nitrobenzene, and carbon disulfide. The small $V_1A_{12}$ value, and consequently the low UCST predicted for the o-dichlorobenzene system, was confirmed by experiment. Carbon disulfide appeared to be the only solvent that did not obey the correlation with $V_1A_{12}$, apparently due to some sort of special interaction present in this case.

In both IPS and PPO gel systems, a decrease in the temperature of phase separation led to a finer microphase separation. Evidently, at lower temperatures the density

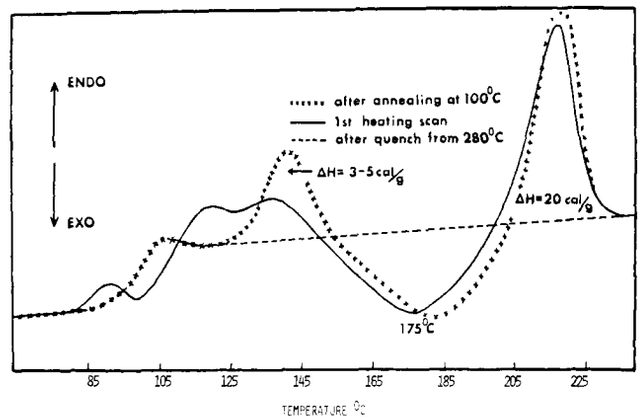


**Figure 3.** DSC scan at 40 °C/min of an IPS glass cast from a 10% gel of the polymer in $CS_2$ at −78 °C.

of crystalline nuclei and/or microphase separated regions is so uniformly high that the polymer chains are immobilized in a three-dimensional network before more extensive domain growth can occur.

**B. Structural Characterization of IPS Gel and Gel Glasses.** DSC scans of 0.16 volume fraction IPS gels showed two endotherms representative of two different crystal size distributions (Figure 2). The sharper higher melting point peak can be assigned to larger crystals which rapidly nucleate at the initial stages of spinodal phase separation when the polymer volume fraction in the polymer-rich phase is low, but large enough so that the critical supercooling for crystallization is achieved. As phase separation proceeds, the local polymer concentration will gradually increase, as will the concentration-dependent supercooling, yielding a broad size distribution of smaller lower melting point crystallites. Of course, the crystallization process will stop when the polymer concentration in most of the domains becomes so high that their $T_g$ reaches the temperature of gelation. This mechanism is confirmed by the rapid onset and broad temperature range of exothermic crystallization observed when a decalin solution of IPS is cooled at 10 °C/min (Figure 2B). The higher-melting crystals can be isolated, for instance in the case of nitrobenzene solutions, by heating the gel to 37 °C to melt the smaller crystals (Figure 2A; dotted line).

A DSC scan of the IPS glass cast from $CS_2$ at −78 °C revealed the presence of a chain reorganization at 90 °C, a $T_g$ at 105 °C, a double endotherm at 119 and 135 °C, and finally an exotherm at 175 °C followed by another larger endotherm at 220 °C (Figure 3). Annealing this material for 50 h at 100 °C lowered the $T_g$ to 95 °C, removed the lower-temperature endotherm, sharpened the high-temperature one, and eliminated the perturbation at 90 °C. The changes induced in the IR spectrum by the annealing treatment were insignificant and suggested an increase in crystal size and or perfection rather than a change in crystal form or chain conformation.

The absolute heat of melting of the smaller endotherm (3–5 cal/g) and its low melting temperature relative to the melting endotherm of the hexagonal crystal form at 220 °C (20 cal/g) indicates that the interchain packing of the gel crystals, phase B, is considerably different from the normal hexagonal crystal form. Since completely disordered IPS melts will not crystallize at 40 °C/min, it is obvious that B crystallites form very effective nucleating sites for the normal crystal form.[21] This recrystallization process does not involve a crystal–crystal transition. The IPS B glass can be heated to 145 °C and quenched to room temperature to a glass that is completely disordered by IR measurement; when the gel is reheated, no low-temper-

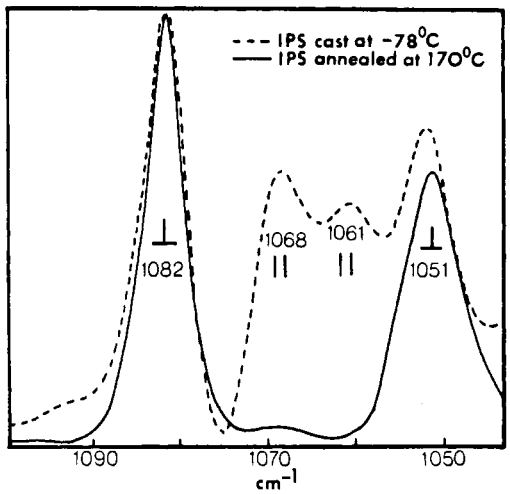


**Figure 4.** 100% crystalline FTIR spectra of the coupled side chain–backbone vibration that is sensitive to the conformation changes in IPS glasses.

ature endotherm appears. However, a rapid crystallization into the normal crystal form ensues just as before when the gel is heated to 160 °C. This result suggests that by using structure B as an intermediate state, it might be possible to form a disordered glass with enhanced parallelism between chains. Such a structure would be an important variant to be used in the structure–property relationships in amorphous glasses. Heating the gel glass to 280 °C destroys all order, and when the gel glass is reheated the DSC scan is typical for a disordered system (Figure 3, dashes).

The infrared spectrum of structure B, the ordered portion of the gel glass into which 40–50% of the polymer was packed, showed numerous bands which were not present in the spherulitically crystallized material which consists of crystals with a $(tg)_3$ ($t$ for trans and $g$ for gauche) chain conformation.[14] Although the subject of the IR spectrum of structure B is considered in greater detail in a later paper,[15] Figure 4 is included in order to show the structural difference.

In APS, the $V'_{18B}$ ($B_1$) aromatic C–H in-plane vibration appears as a singlet at 1070 $cm^{-1}$. By organizing the crystals with $(tg)_3$ sequences characteristic of the $3_1$ helix, we can split the singlet into a doublet due to mixing with backbone CH and $CH_2$ bending vibrations.[16] Both the orientation of the phenyl ring and the conformation of the backbone determine the splitting. The dotted line in Figure 4 shows two doublets for structure B in this frequency regime; the presence of the perpendicular polarized (1082, 1051 $cm^{-1}$) pair indicates that $tg$ diads are present (compare with solid line) while a different, as yet unknown, chain conformation must be responsible for the parallel polarized (1068, 1061 $cm^{-1}$) doublet.

If each conformation existed by itself in separate crystals, the ratio of the IR bands characteristic for each would be temperature dependent. However, since the ordered part of the IR spectrum of both decalin and $CS_2$ gel glasses is the same, both $tg$ and the unknown conformation must together make up one unique helix in one type of crystal.

Flat-plate X-ray photographs of unoriented gel glasses cast from decalin at 0 °C revealed the presence of $d$ spacings at 4.8, 5.1, and 10.3 Å; glasses cast from nitrobenzene at 5 °C had an additional spacing at 20.3 Å. These values are in substantial agreement with these found by Atkins et al.[17] for the IPS–decalin system; they assigned the 5.1 Å reflection to an intrachain scattering and the 10.3 Å spacing to an intermolecular scattering. X-ray line broadening measurements showed that the microcrystallites formed in nitrobenzene were ca. 100 Å in the chain direction and 50 Å perpendicular to this direction. The crystals in the decalin-cast material were substantially smaller, being only 25 Å perpendicular to the chain direction and ca. 100 Å in the chain direction, in agreement with Girolamo et al.,[4] who postulated the existence of fringed micelle crystals in this solvent system. This difference in morphology is reflected in the higher gel crystal melting point of the nitrobenzene cast material (137 °C vs. 107 °C). The relatively higher proportion of higher melting point crystals found for nitrobenzene gels (Figure 2A vs. Figure 2B) also suggests a larger average crystal size. Apparently the crystallite size can be controlled quite precisely on a very small size by changing the gelation solvent.

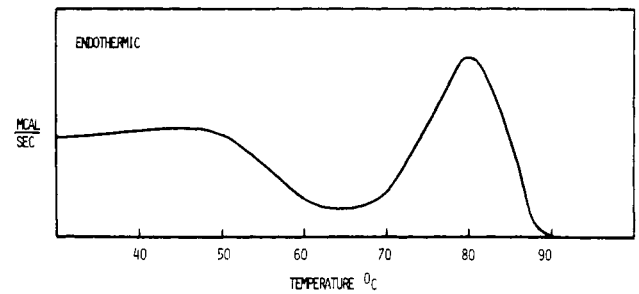


**Figure 5.** DSC scan at 20 °C/min of a 0.16 volume fraction PPO–1-chloronaphthalene gel (endothermic above abscissa).

Table II
Correlation of PPO Gel Crystallization with Phase Separation[a]

| solvent | $V_1A_{12}$ | $T_{GEL}$, °C | | $T_M$, °C |
|---|---|---|---|---|
| (1) nitrobenzene | 1391 | 50 | VCL | |
| (2) pinene | 1272 | 70 | VCL | |
| (3) decalin | 1178 | 70 | VCL | |
| (4) aniline | 768 | 25 | VCL | |
| (5) benzaldehyde | 765 | 25 | VCL | |
| (6) acetophenone | 558 | 25 | VCL | |
| (7) benzonitrile | 492 | 25 | VCL | |
| (8) 1-bromo-naphthalene | 42 | 25 | SCL | 110 |
| (9) 1-chloro naphthalene | | 25 | C | 86 |
| (10) o-dichloro-benzene | 11 | sol to (−17 °C) | | |
| (11) carbon disulfide | 462 | −78 | SCL | 0 |

[a] $V_i$ = molar volume ($cm^3$/mol). $A_{12} = (\delta_{DS} - \delta_{DP})^2 + (1 - Q)(\delta_{AS} - \delta_{AP})^2$, S = solvent, P = IPS, PPO polymer. $T_{GEL}$ is the temperature at which gelation is instantaneous. $T_M$ is the melting point. Sol to ($T$) is the solution that remained mobile and clear until $T$. VCL is a very cloudy gel; SCL is a slightly cloudy gel; and C is a clear gel.

**C. Structural Characteristics of PPO Gels and Gel Glasses.** When a 0.16 volume fraction PPO–1-chloronaphthalene gel is heated, two endotherms appear in the DSC scan (Figure 5). Thus, from all appearances, the mechanism of phase separation and crystallization here is quite similar to that which occurs in PS solutions. Clear PPO gel glasses cast from these gels were studied the most extensively.

Table III shows the X-ray $d$ spacings obtained from two types of glasses that had been solvent exchanged with either acetone or hexane subsequent to vacuum evaporation of the α-chloronaphthalene at room temperature for ca. 2 weeks. The calculated $d$ spacings with which these glasses have been compared are derived from a tetragonal

Table III
X-ray $d$ Spacings from a PPO Glass Cast from a 10% Solution in 1-Chloronaphthalene Which Had Been Gelled at 0 °C

| $hkl$ | $D^o$(acetone), Å | $D^o$(hexane), Å | $D^c$, Å |
|---|---|---|---|
| 001 | 18.0 (m) | | 17.1 |
| 100 | 11.0 (m) | 11.3 (m) | 11.9 |
| 110 | 8.3 (m) | | 8.4 |
| 111 | 8.1 (m) | | 7.6 |
| 102 | 6.5 (m) | 6.9 (s) | 6.9 |
| 200 | 6.0 (m) | | 6.0 |
| 211 | 5.2 (w) | 5.3 (m) | 5.1 |
| 212 | 4.6 (w) | | 4.5 |
| 221 | 4.1 (w) | 4.1 (m) | 4.1 |
| 310 | 3.7 (w) | | 3.8 |
| 320 | 3.4 (w) | | 3.3 |
| 321 | 3.1 (w) | 3.1 (m) | 3.2 |
| $T_M$ | 240 °C | 175 °C | |
| crystal size[a] | | 30 × 30 | |

[a] Length times width.

cell with $a = b = 11.9$ Å and $c = 17.1$ Å,[18,19] in which the PPO chain is proposed to form a $4_1$ helix. Both the hexane and acetone exchanged material seem to belong to the same unit cell, but the larger number of reflections present in the acetone-treated material indicates that the polymer chains within its crystals are more disordered. The presence of the unallowed 001 reflection lends credence to this proposal; this reflection also appears when the solvent originally included in the lattice is removed from PPO single crystals precipitated from α-pinene solution.[18] Crystal sizes of 20–30 Å have been measured by X-ray line broadening for the hexane-treated glass.

The difference in the structure of the two glasses is reflected in their melting points; the hexane-treated glass melts at 170 °C, while the acetone-treated glass melts at the usual melting point of ca. 250 °C. What is particularly puzzling is that the material which we have postulated to be more highly ordered on the basis of X-ray measurements melts considerably below the usual $T_g$ of 220 °C. Infrared measurements on this glass indicate that the residual solvent content is less than 1% and therefore could not be significantly affecting the thermal properties of the PPO. This structure is quite persistent in that a broad endotherm localized between 100 and 200 °C can still be seen after annealing it for 15 min at 300 °C. The endotherm disappears coincidentally with the appearance of the normal $T_g$ only after drastic annealing for 45 min at 300 °C. If the original hexane-treated glass is extracted with acetone before the DSC run, the normal melting point (250 °C) is found. Annealing this material for only 1 min at 300 °C is sufficient to destroy all structure and to generate a $T_g$ at 220 °C. Visual inspection of the glass both before and after acetone treatment reveals no differences in clarity.

As expected from previous work,[20] crystallization induced significant changes in both the asymmetric ether stretch at 1188 $cm^{-1}$ and in the symmetric and asymmetric C–H out-of-plane bends at 858 $cm^{-1}$. Just as in the cases of single crystals from pinene and a complex from $CH_2Cl_2$, the ether stretch shifted to higher frequency in both acetone- and hexane-treated glasses formed from α-chloronaphthalene gels and from a 50/50 mixture of nitrobenzene and $m$-dibromobenzene (Figure 6). A mechanism for this effect has been proposed.[20] The C–H out-of-plane bends in the gel-crystallized material behaved quite differently from those in the crystals precipitated from pinene and $CH_2Cl_2$ (Figure 7). All the gel glasses exhibited a new band at 825 $cm^{-1}$ in addition to the one

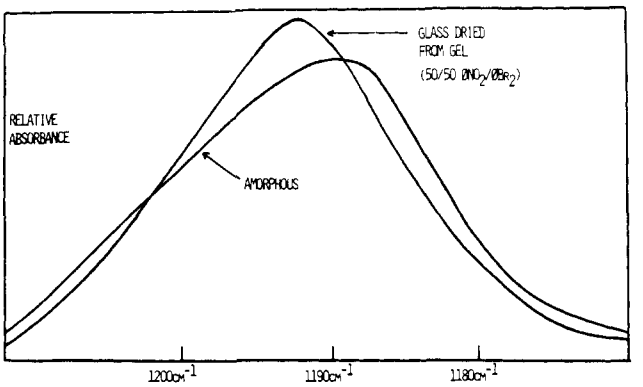


**Figure 6.** Crystallization-induced frequency shift in the C–O–C asymmetric stretch vibration of PPO.

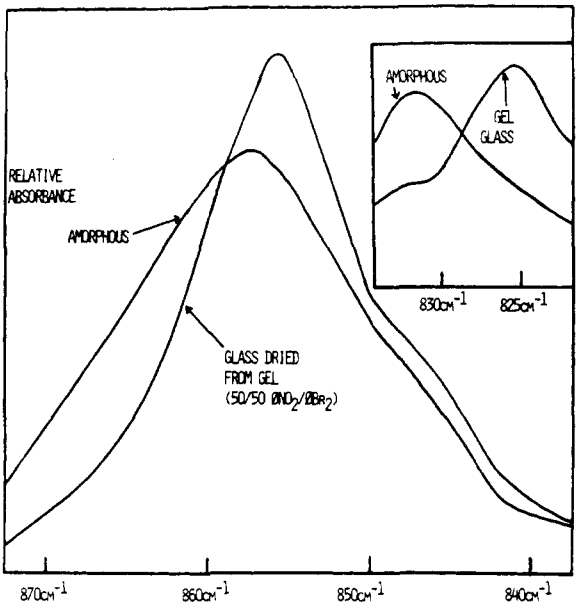


**Figure 7.** Crystallization-induced frequency shift in the C–H out-of-plane vibration of PPO.

usually present at 832 $cm^{-1}$. Amorphous polymer and crystals prepared from pinene and $CH_2Cl_2$ did not have the 825 $cm^{-1}$ band either in the dry or wet state. In addition, the splitting of the 858-$cm^{-1}$ band that was observed for the wet pinene and $CH_2Cl_2$ precipitants was not apparent in the gel-crystallized glasses. However, there was a significant intensification of this band relative to the completely amorphous glass.

**D. Structural Characteristics of 2MPPO–PS Gel Glasses.** Since one of the principal goals of this project is to study the effect of conformation and packing modification on the mechanical properties of polyblends of PPO with polystyrene derivatives, co-casting IPS and PPO from a number of solvents was employed in the attempt to produce structure B in compatible mixtures with PPO. Optically clear gels in which the IPS component has been ordered can be made by gelling at −5 °C from a 50/50 mixture of nitrobenzene and $m$-dibromobenzene and subsequently increasing the temperature to 35 °C to eliminate any IPS phase separation that might have occurred at lower temperature. The solvent is then removed to yield transparent films. Figure 8 shows how the IPS helix-sensitive region at 930–890 $cm^{-1}$ in these blend glasses reacts to blend composition. A significant reduction in the structure B helix band at 916 $cm^{-1}$ occurs at high PPO contents. It is important to note that even though blending with PPO appears to retard the formation of structure B,

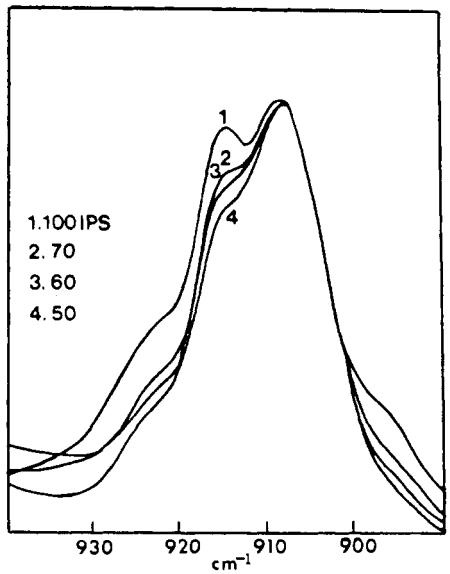


**Figure 8.** FTIR spectra indicating the presence of structure B of IPS in PPO–IPS blend glasses cast from a 16% polymer gel in a 50/50 mixture of nitrobenzene and *m*-dibromobenzene.

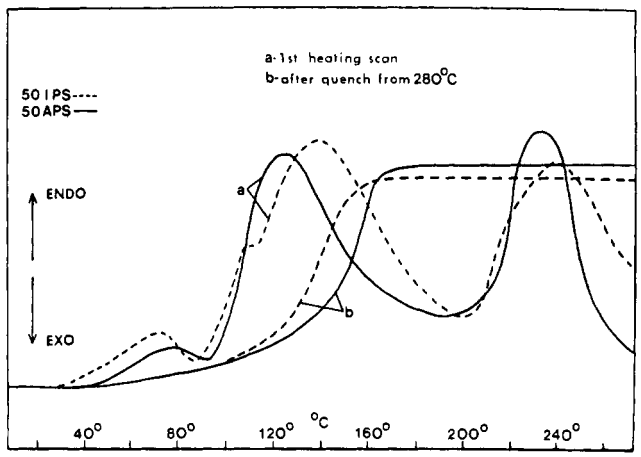


**Figure 9.** DSC scans at 40 °C/min of 50/50 PPO–IPS or APS blend glasses cast from a 16% polymer gel in a 50/50 mixture of nitrobenzene and *m*-dibromobenzene.

significant amounts of this structure are still formed in the 90–50% IPS range where the brittle to ductile transition takes place in unordered IPS–2MPPO blends.[22] Thus we have a useful structural tool in the range of critical compositions.

Figure 9 shows that even though there is no visible phase separation (>1000 Å), microscopic phase separation occurs initially in this blend system. This conclusion follows from the fact that the $T_g$ of the blend has not increased above that of pure IPS at 100 °C. When the blend is heated above $T_g$, the IPS crystals melt out and subsequently mix with amorphous PPO. Above 200 °C, another endotherm is encountered which we assign to the melting of small PPO gel crystallites. This hypothesis is confirmed by the presence of two endotherms in the dilute solution (Figure 10).

The APS–PPO gel glass also appears to be significantly phase separated (Figure 9). The presence of an endotherm at 240 °C shows that the PPO component has crystallized; since the polystyrene is atactic, Figure 9 also suggests that the exotherm at 200 °C could be due to an exothermic reorganization within the PPO crystals and not a polystyrene recrystallization. Both the APS and IPS blends can be significantly homogenized by annealing them slightly above the $T_g$ of PS (Figure 11). Heating the

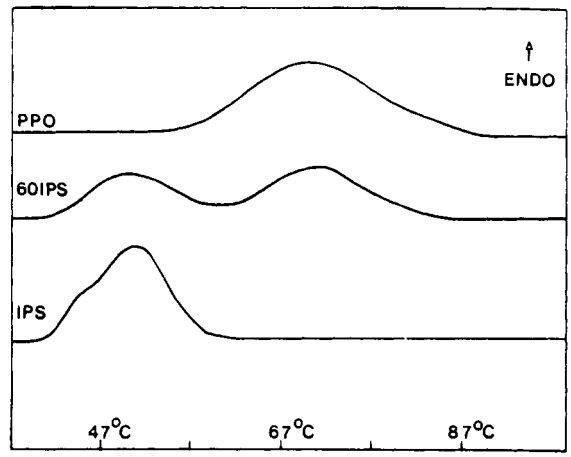


**Figure 10.** DSC scans at 40 °C/min of 10% IPS, 10% PPO, and 16% 60 IPS–40 PPO gels in the same solvent as Figure 9.

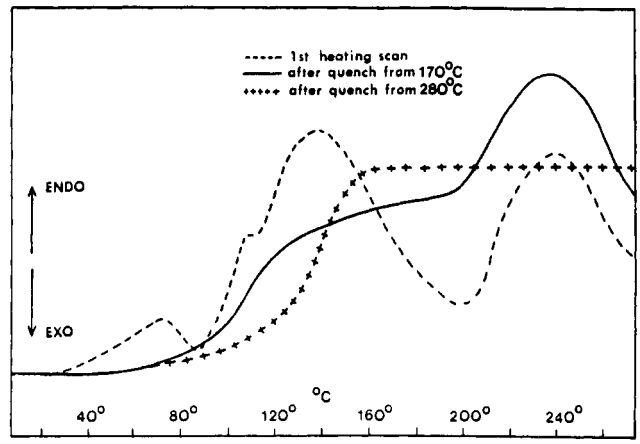


**Figure 11.** Same as Figure 9 except DSC scans of a 50 IPS–50-PPO glass only.

blends to 280 °C induces complete mixing of the PPO and PS components and yields an amorphous glass with an intermediate $T_g$.

Significantly better mixing of the two polymer components can be achieved by gelling the PPO component of an APS–PPO solution in α-chloronaphthalene at 25 °C, vacuum drying, and extracting with hexane. A 50/50 blend is quite clear and has a $T_g$ at 120 °C and a broad 2MPPO melting endotherm from 160–210 °C (Figure 11). In this solvent, significant spinodal domain growth of the PPO component does not prevent mixing of these domains with the APS as the solvent is removed. Apparently, mixing of the two polymers is prevented only when both PS and PPO undergo phase separation, as for instance in the nitrobenzene–*m*-dibromobenzene system.

## IV. Conclusions

Spinodal phase separation of sufficiently concentrated solutions of APS will yield gels which consist of a continuous network of polymer-rich phase cross-linked by glassy microdomains. Solutions of IPS and 2MPPO which can phase separate by the same spinodal mechanism formed gels which were cross-linked by both glassy microdomains and 20–100 Å fringed micelle crystallites. A broad bimodal distribution in crystallite size was due to the rapidity of phase separation and the large local concentration excursions experienced by the solution. An attempt to use solubility parameters to predict the microphase separation and gel crystallization temperatures of IPS solutions led to the conclusion that dispersion forces

are the ones which predominantly control the solution behavior of these systems.

In agreement with Overbergh et al.,[21] we have determined that the IPS gel crystals consist of a high-energy conformational variant of the usual isotactic configuration. The normal $4_1$ helical tetragonal form of PPO was found in its gel crystals. Crystal size and perfection and microphase separation in glasses of PS, PPO, and their blends cast from gel solutions were affected by gelation solvent and annealing treatment.

The microheterogeneities within these glasses should have a significant effect upon plastic microdeformation morphology. With the structural characterization of these materials in hand, subsequent reports will attempt to explore structure–property relationships of these materials. The "critical" microheterogeneity size responsible for crazing and localized microshear banding will be of special interest.

**Acknowledgment.** The authors wish to acknowledge support of this work by the NSF through Grant DMR 76-80710-A01. Special thanks are due to Professor Andrew Keller who initially encouraged us to study this problem and who since has made many valuable suggestions. We would also like to acknowledge the helpful discussions we had with Professor Paul Painter on the interpretation of the FTIR results on IPS gels.

## References and Notes

(1) J. W. Cahn, *J. Chem. Phys.*, **42** (1), 93 (1965); *Trans. Am. Inst. Min., Metall. Pet. Eng.*, **242**, 166 (1968).
(2) L. D. Grandine and J. Ferry, *J. Appl. Phys.*, **24** (6), 679 (1953).
(3) A. A. Tager, V. E. Dreval, M. S. Lutsky, and G. V. Vinogradov, *J. Polym. Sci., Part C*, **23**, 181 (1968).
(4) M. Girolamo, A. Keller, K. Miyasaka, and N. Overbergh, *J. Polym. Sci., Polym. Phys. Ed.*, **14**, 39 (1976).
(5) D. R. Paul, *J. Appl. Polym. Sci.*, **11**, 439 (1967).
(6) G. S. Y. Yeh, *Crit. Rev. Macromol. Sci.*, **1** (2), 1973 (1972).
(7) "Polymer Handbook", J. Brandup and E. H. Immergut, Eds., Wiley, New York, 1975.
(8) P. J. Flory, "Principles of Polymer Chemistry", Interscience, New York, 1953.
(9) Y. Izumi and Y. Miyake, *Polym., J.*, **3**, 647 (1972).
(10) C. M. Hansen, *J. Paint Technol.*, **39** (505), 104 (1967).
(11) S. H. Maron and F. E. Filisko, *J. Macromol. Sci., Phys.*, **6**, 57 (1970).
(12) M. Kobayashi, K. Tsumura, and H. Tadokoro, *J. Polym. Sci., Part A-2*, **6**, 1493 (1978).
(13) M. Kobayashi, K. Akita, and H. Tadokoro, *Makromol. Chem.*, **118**, 324 (1968).
(14) G. Natta, P. Corradini, and I. W. Bassi, *Nuovo Cimento, Suppl.*, **15**, 68 (1960).
(15) S. Wellinghoff and Eric Baer, to be published.
(16) P. Painter and J. L. Koenig, *J. Polym. Sci., Polym. Phys. Ed.*, **15** (11), 1885 (1977).
(17) E. D. Atkins, D. H. Isaac., A. Keller, and K. Miyasaka, *J. Polym. Sci., Polym. Phys. Ed.*, **15**, 211 (1977).
(18) J. M. Barrales-Rienda and J. M. G. Fatou, *Kolloid Z. Z. Polym.*, **244**, 317 (1971).
(19) A. Factor, G. E. Heinshon, and L. H. Vogt, Jr., *J. Polym. Sci., Part B*, **7**, 205 (1969).
(20) S. Wellinghoff, J. L. Koenig, and Eric Baer, *J. Polym. Sci., Polym. Phys. Ed.*, **15** (11), 1913 (1977).
(21) N. Overbergh and H. Berghmans, *Polymer*, **18**, 883 (1977).
(22) S. Wellinghoff and Eric Baer, *J. Appl. Polym. Sci.*, **22**, 2025 (1978).
(23) "International Critical Tables", Vol. 5, 1929, p 157.
(24) R. Foster, "Organic Charge-Transfer Complexes", Academic Press, New York, 1969.

# Fast Neutron Irradiation Effects on Polymers. 1. Degradation of Poly(methyl methacrylate)

**Shigenori Egusa,[1] Kenkichi Ishigure, and Yoneho Tabata***

*Nuclear Engineering Research Laboratory, The University of Tokyo, Tokai-mura, Ibaraki 319-11, Japan.* *Received April 10, 1979*

ABSTRACT: Irradiation effects of fast neutrons on poly(methyl methacrylate) were compared with those of $^{60}$Co $\gamma$ rays from the viewpoint of linear energy transfer (LET). The $G$ value of main-chain scissions, $G$(S), and the change in the molecular weight distribution of irradiated polymers were determined by means of gel-permeation chromatography. The LET dependence of $G$(S) is definite for in-vacuo irradiations [$G\gamma^{vacuo}$(S) = 1.54 ● 0.11 for $^{60}$Co $\gamma$ rays (LET: ca. 0.02 eV/Å) and $G_n^{vacuo}$(S) = 1.04 ± 0.13 for fast neutrons (LET: ca. 3.7 eV/Å)], but the dependence is not so definite for in-air irradiations [$G_\gamma^{air}$(S) = 0.73 ± 0.06 and $G_n^{air}$(S) = 0.66 ± 0.10]. The plot of the $M_w/M_n$ ratio vs. the number of main-chain scissions deviates from that predicted by the random-degradation theory. The deviation is more distinct for fast-neutron than for $\gamma$-ray irradiations. The reduced $G$(S) value and the enhanced deviation from the random degradation at high LET are attributable to the increased inhomogeneity of microscopic energy deposition. A parameter expressing the microscopic inhomogeneity, $\Delta D/x$, is introduced in the computer simulation of the nonrandom degradation and is adjusted so as to give the best fit between the observed and simulated plots of the $M_w/M_n$ change. The computer simulation gives the $\Delta D/x$ value of 1.54 and 0.52 Mrad for fast-neutron and $\gamma$-ray irradiations, respectively, indicating that the $\Delta D/x$ ratio (ca. 3) is strikingly small compared with the LET ratio (ca. 180).

Fast-neutron and $^{60}$Co $\gamma$-ray irradiations on polymers will produce different effects not only in the efficiency of main-chain scission, cross-linking, etc., but also in the molecular weight distribution change. The different effects are considered to arise from a difference in linear energy transfer (LET) between recoil protons and secondary electrons which are produced by the interaction of atoms with fast neutrons and $\gamma$ rays, respectively. The LET difference will produce differences in the spatial distribution of energy deposition[2,3] and, consequently, in the spatial distribution of reactive species such as macroradicals and low molecular weight free radicals. Several authors have carried out the ESR study on the spatial distribution of free radicals trapped in matrices such as poly(methyl methacrylate) (PMMA),[4,5] glassy methanol,[6] and *n*-eicosane single crystal[7,8] irradiated with different types of radiation such as protons from an accelerator and $^{60}$Co $\gamma$ rays. Kaul and Kevan[5] found that the local spin

0024-9297/79/2212-0939$01.00/0 